The vulnerable artery: early and rapid deposition of lipid in coronary arteries is associated with subsequent development of thin-cap fibroatheromas

Matthew D. Saybolt[1], MD; Scott M. Lilly[1], MD, PhD; Dhavalkumar Patel[1], MD, MPH; Damir Hamamdzic[1], DVM, PhD; Raul Llano[1], MD; Robert S. Fenning[1], MD; Sean Madden[2], PhD; Robert L. Wilensky[1]*, MD

1. Cardiovascular Division, Hospital of the University of Pennsylvania, Philadelphia, PA, USA; 2. InfraReDx, Inc., Burlington, MA, USA

KEYWORDS

Abstract

Aims: We aimed to determine whether intravascular ultrasound (IVUS) and near infrared spectroscopy (NIRS) could identify arteries which would subsequently develop a thin-cap fibroatheroma (TCFA).

Methods and results: Three-vessel angiography, IVUS and NIRS evaluations were performed at three, six and nine months after induction of diabetes mellitus and hypercholesterolaemia in 13 Yorkshire pigs (n=37 arteries). *In vivo* total arterial plaque plus media (P+M) area, echo-attenuated plaque (AP) area by IVUS, and lipid core burden index (LCBI) by NIRS were compared to histology at nine months. P+M mean area increased over time (3 vs. 6 months p<0.01; 6 vs. 9 months p<0.01), as did the AP area and mean LCBI between three and six months (p<0.01). There were 69 TCFAs within 18 arteries. The mean LCBI at six months was greater in arteries containing a TCFA (77.8±17.4 vs. 34.3±11.4; p=0.04) as was the ΔLCBI from three to six months (55.3±16.9 vs. 3.3±16.0; p=0.03). Arteries which contained TCFA at nine months had greater AP area by IVUS at six months (p=0.007).

Conclusions: The early and persistent accumulation of total arterial lipid detected by NIRS was associated with the future development of TCFAs.

*Corresponding author: Hospital of the University of Pennsylvania, 3400 Spruce Street, 9 Gates, Philadelphia, PA, 19104, USA.
E-mail: Robert.wilensky@uphs.upenn.edu

Abbreviations

AP	attenuated plaque
DM	diabetes mellitus
HC	hypercholesterolaemia
IVUS	intravascular ultrasound
LCBI	lipid core burden index
NIRS	near infrared spectroscopy
P+M	plaque plus media
TCFA	thin-cap fibroatheroma
ThCFA	thick-cap fibroatheroma

Introduction

Rupture of a thin-cap fibroatheroma (TCFA) is the dominant mechanism underlying acute coronary syndromes and ischaemic sudden death[1]. TCFAs possess a thin fibrous cap infiltrated by macrophages with rare smooth muscle cells, overlying a large necrotic

Editorial, see page 1574

core[1]. Coronary angiography cannot effectively identify histological hallmarks of high-risk lesions with a propensity for future instability. However, invasive diagnostic systems can lend insight into plaque structure, composition, and haemodynamic significance.

By measuring the wavelength-dependent interaction of electromagnetic radiation with matter, near infrared spectroscopy (NIRS) can measure the unique chemical signatures in tissue. The variable absorption and scattering tissue properties at various wavelengths yield a spectroscopic signature that can identify specific tissue compositions. Early work in the field demonstrated that NIR spectra could accurately characterise low-density lipoprotein cholesterol, cholesterol, and cholesterol esters in both animal models and humans[2]. Intravascular NIRS (InfraReDx Corp, Burlington, MA, USA) identifies lipid deposition within the arterial wall and has been shown to determine the presence of lipid core plaques accurately[3].

We have previously demonstrated that the combination of NIRS and intravascular ultrasound (IVUS) detects and localises the presence of a high-risk coronary fibroatheroma, demonstrating increased inflammation and cellular apoptosis within the fibrous cap in diabetic/hypercholesterolaemic (DM/HC) pigs[4]. However, the rate of lipid accumulation at the arterial level and its relationship to the future development of TCFAs within that artery are unknown. An understanding of the development and natural history of the vulnerable artery may ultimately provide an improved ability to risk stratify patients, measure vascular response to novel pharmaceutical agents, and aid in targeting those arteries with an increased propensity for TCFA development. Hence, the goal of the current study was to identify vulnerable arteries which would develop TCFAs. The DM/HC porcine model, which develops high-risk human-like atherosclerotic lesions, was employed[5,6], and progression of atherosclerosis was measured by IVUS and lipid deposition by NIRS.

Methods

ANIMAL MODEL

Invasive studies were performed in 13 male DM/HC-induced Yorkshire swine (25-30 kg; Archer Farms, Darlington, MD, USA) **(Figure 1)**. DM, defined as a consistent blood glucose level >150 mg/dL, was successfully induced and maintained with a single intravenous injection of 125 mg/kg of the β-cell cytotoxin streptozotocin (Sicor Pharmaceuticals, Irvine, CA, USA). Animals were fed a diet containing 0.5% cholesterol, 5% lard and 1.5% sodium cholate (Animal Specialties and Provisions Inc., Quakertown, PA, USA) to achieve hypercholesterolaemia. Serum glucose and cholesterol levels and weight were monitored throughout the study. To reduce the risk of ketoacidosis, insulin was administered when the serum glucose level was >350 mg/dL[6]. The study was approved by the Institutional Animal Care and Use Committee (IACUC) of the University of Pennsylvania.
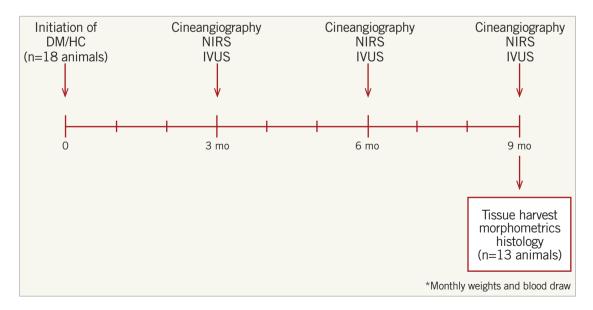

Figure 1. *Study design. DM/HC: diabetes mellitus/hypercholesterolaemia; IVUS: intravascular ultrasound; NIRS: near infrared spectroscopy*

IMAGING PROTOCOLS (APPENDIX)

Multivessel serial diagnostic coronary artery evaluation was performed at three, six and nine months following DM/HC induction. Animals were medicated with ketamine (2 mg/kg), medetomidine (0.1 mg/kg), atropine (0.04 mg/kg) and isofluorane to induce and maintain anaesthesia. Clopidogrel (75 mg) and aspirin (325 mg) were administered for three days prior to and continued for two days following intravascular procedures. Periprocedural intravenous heparin was administered to achieve an activated clotting time of >300 seconds. Selective cineangiography of the left and right coronary arteries was performed in two views before and after IVUS (Boston Scientific Corporation, Marlborough, MA, USA) and NIRS pullbacks were performed to identify and standardise imaging start and endpoints. The IVUS catheter was advanced to a distal side branch, the location noted, and a motorised pullback to the aorto-ostial junction was performed at a constant speed of 0.5 mm/s. A 3.2 Fr NIRS catheter was advanced to the identical distal side branch and spectral data were collected during automated motorised pullback to the ostium at 0.5 mm/s and 240 rpm.

TISSUE RETRIEVAL AND HISTOLOGICAL ANALYSIS (APPENDIX)

Following the nine-month *in vivo* evaluation, the animals were sacrificed with intravenous pentobarbital. The heart was rapidly removed and the coronary arteries were perfused at physiologic pressure with saline and then for >2 hours with 10% neutral buffered formalin. The arteries were cut into 5 mm blocks, with the distal ends marked and proximal ends sectioned for histology.

Statistical analysis

Comparison of continuous variables for two unmatched groups based on the presence or absence of TCFA was performed using univariate analysis of variance. Continuous variables measured over time (three, six and nine months) were analysed in pairwise fashion with analysis of variance. All p-values presented are two-tailed, and <0.05 was considered statistically significant. Analyses were performed with Stata 12.0 software (Stata Corp, College Station, TX, USA).

Results

Results are shown for the 13 animals which underwent three invasive evaluations yielding 37 evaluated arteries. Following induction, there was a rapid rise in serum glucose and cholesterol levels with sustained elevations **(Figure 2)**. A per-vessel IVUS analysis demonstrated a significant increase in P+M area at six- and nine-month time points (p<0.01). AP area increased from three to six months (p<0.01), remaining stable from six to nine months. Mean LCBI was 33.2±5.4, 55.5±10.8, and 52.1±8.0 at three, six, and nine months, respectively (3 vs. 6 months p=0.003; 6 vs. 9 months p=0.41) **(Table 1)**. As animals grew, many coronary arteries lengthened. From six to nine months, 19 of the 37 arteries increased in length. Originally, 18 animals underwent DM/HC
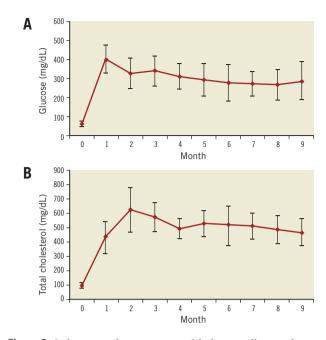
Figure 2. *Induction and maintenance of diabetes mellitus and hypercholesterolaemia. Glucose (A) and total cholesterol (B) over time (mean±standard deviation).*

induction. Five died unexpectedly secondary to ischaemic sudden death, four of which demonstrated multivessel disease with superimposed thrombus.

Twenty-eight arteries contained a fibroatheroma (TCFA or ThCFA, n=137 sections) and nine did not. There was a mean of 4.9±3.2 histologic sections containing a fibroatheroma per artery, of which 2.5±3.1 were TCFAs. Arteries demonstrating a fibroatheroma had a significantly greater increase in LCBI between three and nine months (35.0±12.4 vs. 5.0±11.0, respectively; p=0.046). The nine-month LCBI was also higher among the vessels that contained a fibroatheroma (62.5±10.3 vs. 25.6±6.7; p=0.004). Intra-animal heterogeneity was evidenced in that four animals developed fibroatheromas in only one or two coronary arteries.

As TCFAs represent a higher-risk phenotype, we focused our analysis on their development. By histology, 18 arteries (69 sections) contained a TCFA possessing an average cap thickness of 65.6±23.9 μm. By IVUS, 52 TCFAs demonstrated negative remodelling at nine months (75.4%). The mean coronary artery P+M and AP areas based on the presence or absence of TCFA at nine months are shown in **Figure 3**. Mean P+M area increased in

Table 1. Per-vessel analysis.

	3 months	6 months	9 months
Total plaque+media area (mm²) (IVUS)	48.9±26.9	250.4±182.7*	449.0±471.8*
Total attenuated plaque area (mm²) (IVUS)	0	16.2±28.0*	29.0±48.8
Lipid core burden index (NIRS)	33.2±5.4	55.5±10.8*	52.1±8.0
Thirteen animals (n=37 vessels) mean LCBI by NIRS, total plaque plus media area, and total echo-attenuated plaque area by IVUS at three, six, and nine months. Plaque+media area, and attenuated plaque area are the mean±standard deviation while LCBI values are the mean±standard error of the mean. *p<0.01			

TCFA-containing arteries from 50.4±26.8 mm^2 at three months, to 303.1±215.0 mm^2 at six months, and 583.7±583.4 mm^2 at nine months (3 vs. 6 months p=0.098; 6 vs. 9 months p=0.09). Arteries which contained a TCFA at nine months had a highly significant increase in AP area by IVUS from three to six months (0.0 mm^2 vs. 28.9±35.6 mm^2; p=0.007) and a non-significant increase from six to nine months (28.9±35.6 mm^2 vs. 43.0±43.8 mm^2; p=0.09). In arteries in which TCFAs were absent, there was no change in mean P+M or AP areas between three and nine months **(Figure 3)**.

The LCBI increased significantly in arteries containing ≥1 TCFA between three and six months (p=0.04), and remained stable between six and nine months (p=0.46). Notably, arteries that did not develop a TCFA (n=19) displayed similar LCBIs at all three time points **(Figure 4)**. Compared to vessels in which a TCFA was absent at nine months, TCFA-containing arteries had a significantly greater mean LCBI (p=0.04) and mean ΔLCBI (p=0.03), respectively, at six months **(Table 2)**. Chemograms of an artery which went on to develop multiple TCFAs and an artery which did not, along with corresponding histology at nine months, are displayed in **Figure 5**. The four animals excluded from the primary analysis which died suddenly from ischaemic sudden death

Figure 4. *Early increase in lipid core burden index is associated with TCFA development. A) LCBI over time of arteries in which a TCFA was present at nine months (n=18). B) Arteries without a histologic TCFA (n=19). Mean±standard error of the mean plotted against time. LCBI: lipid core burden index*

were found to have multivessel disease with superimposed thrombus at necropsy. The chemograms of arteries from two animals which died suddenly before the six-month evaluation, along with corresponding histology, are displayed in **Appendix Figure 1** and **Appendix Figure 2**, respectively, one demonstrating a thrombus which led to witnessed sudden death.

In 11 of the 18 TCFA-containing arteries, the LCBI increased from three to six months and remained stable from six to nine months. In a subgroup analysis of these 11 arteries, AP area increased from six to nine months in seven arteries. Additionally, a comparison of calcification and AP area at six and nine months demonstrated no significant difference in mean percent
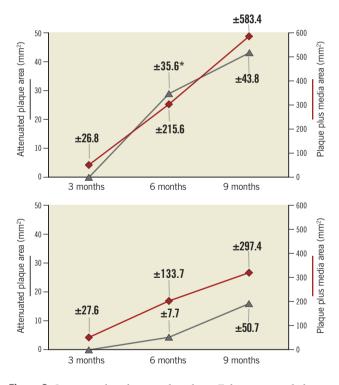
Figure 3. *Intravascular ultrasound analysis. Echo-attenuated plaque and total arterial plaque+media areas by IVUS at three, six and nine months after DM/HC induction, based on the presence (A) or absence (B) of a thin-cap fibroatheroma at nine months by histology. The mean arterial attenuated plaque areas (grey line) are on the left-hand ordinate and mean arterial plaque+media area (red line) on the right-hand ordinate. Data point labels indicate standard deviation. Attenuated plaque area only increased significantly from three to six months in arteries which contained TCFA at nine months (*p=0.007).*
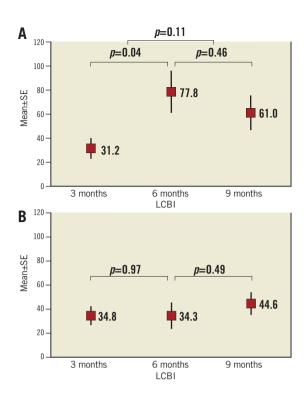
Table 2. NIRS analysis.

	TCFA+arteries (n=18)	TCFA–arteries (n=19)	*p*-value
LCBI (3 months)	31.2±8.4	34.8±7.3	0.75
LCBI (6 months)	77.8±17.4	34.3±11.4	0.04
LCBI (9 months)	61.0±14.3	44.6±9.5	0.34
ΔLCBI 3 to 6 months	55.3±16.9	3.3±16.0	0.03
ΔLCBI 3 to 9 months	−16.8±26.5	10.3±14.6	0.37

Arteries containing a TCFA at nine months were compared to those in which TCFAs were absent at nine months. Values represent mean±standard error of the mean.
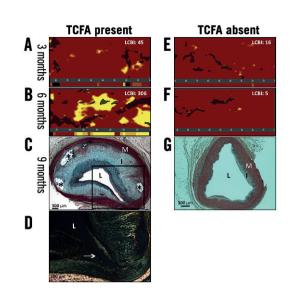
TCFA present | **TCFA absent**

A (3 months) — LCBI: 45
B (6 months) — LCBI: 306
C (9 months)
D

E — LCBI: 16
F — LCBI: 5
G

Figure 5. *Comparative chemograms and histology of an artery which developed a TCFA versus one that did not develop a fibroatheroma. A) & B) Chemograms at three and six months of a TCFA-containing artery at nine months. The probability of lipid core plaque at the region of interest is displayed by using a colour scale where each pixel marked red indicates low probability and each yellow pixel a high probability. The black pixels of the chemogram are interference from the guidewire. The block chemogram is shown beneath each quantitative chemogram. There is an increase in lipid core plaque and LCBI from three to six months. C) Movat's pentachrome stain of a TCFA from the interrogated artery at nine months. A thin fibrous cap over a dense necrotic core is outlined. D) Photomicrograph of an adjacent section stained with Picro-sirius at higher magnification of the outlined area in panel C. There is an absence of collagen in the fibrous cap (arrow). Under polarised light new collagen appears green while old collagen appears yellow or pink. E) & F) Chemograms and block chemograms at three and six months of an artery in which pathologic intimal thickening was present at nine months (G). The LCBI was stable over time. The artery in panel G has no fibrous cap, thus Picro-sirius red staining was not performed. *calcium deposit; I: intima; L: lumen; M: media*

calcification (6 months: 53.3±27.6% vs. 9 months: 47.4±28.4%, p=0.48), mean calcium index (0.64±0.38 vs. 0.55±0.39, p=0.50), or mean percent AP area (9.4±5.4% vs. 7.7±5.2%, p=0.31). There was a non-significant increase in mean lumen area (6.9±0.94 mm² vs. 8.1±2.3 mm², p=0.17) from six to nine months.

Discussion

This is the first study to compare serial *in vivo* NIRS and IVUS with histological endpoints on a per-vessel analysis. The presented data show an association between early and rapid increases in lipid accumulation and subsequent arterial vulnerability as evidenced by the significant increase in TCFA development. In addition, arteries which developed TCFAs had larger echo-attenuated plaque areas at six months identifying putative necrotic core, a histological hallmark of more severe and higher-risk lesions[7]. Coronary

vessels which did not develop TCFAs demonstrated stable and relatively unchanged LCBIs throughout the study. In addition, 75.4% of histologic TCFAs demonstrated negative remodelling by IVUS. Hence, the rapid increase in arterial lipid deposition as identified by NIRS predicted those vulnerable arteries which subsequently developed a TCFA. As such, this study establishes the time course of TCFA development in this animal model and suggests that the accumulation rate of arterial lipid has important prognostic significance.

Unstable coronary artery disease is a pan-coronary process, often with multiple high-risk lesions present within the same coronary artery. Using angioscopy, Asakura et al observed 3.2±1.7 non-culprit yellow plaques (denoting lipid-rich atheroma) per coronary artery in patients undergoing an evaluation following a myocardial infarction[8]. Ohtani et al, also using angioscopy, demonstrated that a higher number of yellow plaques predicted future development of an acute coronary syndrome (p=0.008). By multivariate analysis, only the number of yellow plaques and the presence of multi-vessel disease were independent risk factors for an acute coronary syndrome[9]. Using OCT, Kubo observed that 38% of patients who suffered a myocardial infarction had additional non-culprit TFCAs vs. 6% of those with stable angina[10].

The present study supports the hypothesis that NIRS may play a role in the early identification of specific arteries with an increased propensity for future TCFA development and/or vulnerability. Assessment of culprit arteries of patients presenting with an acute coronary syndrome with NIRS have yielded similar results. Madder et al showed that non-culprit lipid-rich plaques were observed within the culprit vessel in 73.3% of patients presenting with an acute coronary syndrome, compared to only 17.6% in patients presenting with stable angina (p=0.002). Of patients presenting with an acute coronary syndrome, 84.4% had a target lesion lipid core plaque compared to 52.5% of patients presenting with stable angina[11]. Our findings further add to observations made in human studies of non-culprit arteries assessed by NIRS. Oemrawsingh et al observed prospectively that an elevated NIRS-derived coronary LCBI of non-culprit coronary arteries was associated with a fourfold increase in major adverse cardiac events in the following year[12]. Patients with non-culprit lesion LCBI values equal to or above a median of the sample had a cumulative one-year event rate (all-cause mortality, non-fatal ACS, stroke, and unplanned coronary revascularisation) of 16.7%, and the relationship between LCBI and primary endpoint was similar for stable angina and acute coronary syndrome patients. The current study shows that increased arterial lipid core plaque detected by NIRS is associated with the future development of TCFAs within those arteries leading to increased vulnerability.

We have previously shown, in this model, that NIRS positivity at nine months significantly correlated with the presence, at that point in time, of high-risk fibroatheromas with thinner fibrous caps, increased fibrous cap inflammation and higher rates of apoptosis, all signs associated with increased fibrous cap instability[4]. The current study extends those results by demonstrating that the

rapid increase in lipid is associated with the future development of TCFAs on an arterial basis. Although NIRS can identify lipid-rich plaques, it cannot accurately determine fibrous cap thickness and therefore cannot differentiate between TCFAs and ThCFAs[4]. However, by using NIRS to determine LCBI, it is possible to identify those arteries with a fibroatheroma and/or an increased propensity for developing a TCFA. This would allow one to focus one's attention utilising other technologies such as OCT, specifically to determine fibrous cap thickness and the natural history of such lesions insofar as lesions containing large necrotic cores and thin fibrous caps have an increased risk of future instability[7]. Identifying arteries with an increased propensity for the future development of high-risk lesions may ultimately improve risk stratification in patients in whom escalation of anti-atherosclerotic therapies or selective intervention may be of benefit. Utilising NIRS, Kini et al have demonstrated a reduction in 4 mm maximal segment LCBI in non-target lesions in response to short-term intensive statin therapy[13]. Hence, NIRS may be a valuable objective modality to assess how a diseased coronary artery responds to pharmacotherapy. In addition, PCI of lesions with higher lipid core plaques is associated with a higher risk of periprocedural myocardial infarction[14].

The aetiology of the non-significant decrease in vessel LCBI between six and nine months after induction of DM/HC is unclear. The maximum depth of photon penetration of NIRS within atherosclerotic lesions is unknown, but it is believed to average about 1 mm, reflecting an unavoidable consequence of diffuse reflectance spectroscopy which measures a subtended area of lipid. Thus, decreased photon penetration may result in circumstances in which the NIRS algorithm reports stable or falsely negative LCBI over time in the presence of fibroatheromas with progressively deeper lipid pools, and/or calcified cores, expansive remodelling or in the setting of increasing lumen area. Notably, Gardner et al reported in *ex vivo* human coronary samples that false-negative readings were most frequently produced by lipid cores with extensive calcification and displacement of necrotic core lipid by calcium[3]. However, we did not detect a significant difference in calcification or lumen area by IVUS in TCFA-containing arteries in which the LCBI was stable from six to nine months. Changes in the chemical signature of necrotic cores can also result from a loss of lipid pool from undetected healed ruptures, or as a necrotic core became more necrotic and less lipemic. In a histopathologic correlation study, Pu et al demonstrated that IVUS echo-attenuated plaque had a specificity of 94.7% for the detection of a large lipid/necrotic core. However, there were a number of echo-attenuated plaques which had an LCBI approaching zero[15]. We noted that 19 of 37 interrogated arteries increased in length between six and nine months, of which 11 (of the 19) demonstrated a regression in the LCBI. This indicates that, as animals grew and vessels lengthened, the number of yellow pixels indicating lipid deposition remained relatively stable while the number of red pixels, indicating non-lipemic tissue, proportionally increased, thereby resulting in a reduced total arterial LCBI.

Limitations

Our study is limited by the fact that histology only examined 5 μm sections from a segment 5 mm in length. Given the burden of atheroma measured by IVUS across the study samples and arterial lengths, unexamined sections may have contained high-risk phenotypes. We observed large standard deviations in the mean AP area and P+M area between the two groups from six to nine months. Within individual animals there were arteries in which these values shrank or remained stable, while others had dramatic increases out of proportion to other animals or arteries, reflecting the dynamic nature of high-risk lesions. This has been shown clinically by Kubo et al and Zhao et al[16,17], where phenotypic changes of coronary lesions over time were demonstrated in both stable and unstable non-culprit lesions. As such, the relatively small number of arteries assessed and the large standard deviation of lipid core area could reflect a type 2 error, though the burden of disease detected serially by IVUS and NIRS and histologically at necropsy would suggest otherwise.

Conclusions

The early development and persistence of arterial lipid core plaque between three and six months predicts the presence of at least one TCFA within that artery at nine months.

Impact on daily practice

NIRS LCBI identifies a vulnerable artery at risk for the future development of more clinically significant atherosclerotic lesions.

Acknowledgements

Conflict of interest statement

S. Madden is an employee of InfraReDx. The other authors have no conflicts of interest to declare.

References

1. Virmani R, Burke AP, Farb A, Kolodgie FD. Pathology of the vulnerable plaque. *J Am Coll Cardiol.* 2006;47:C13-8.

2. Caplan JD, Waxman S, Nesto RW, Muller JE. Near-infrared spectroscopy for the detection of vulnerable coronary artery plaques. *J Am Coll Cardiol.* 2006;47:C92-6.

3. Gardner CM, Tan H, Hull EL, Lisauskas JB, Sum ST, Meese TM, Jiang C, Madden SP, Caplan JD, Burke AP, Virmani R, Goldstein J, Muller JE. Detection of lipid core coronary plaques in autopsy specimens with a novel catheter-based near-infrared spectroscopy system. *JACC Cardiovasc Imaging.* 2008;1:638-48.

4. Patel D, Hamamdzic D, Llano R, Patel D, Cheng L, Fenning RS, Bannan K, Wilensky RL. Subsequent development of fibroatheromas with inflamed fibrous caps can be predicted by intracoronary near infrared spectroscopy. *Arterioscler Thromb Vasc Biol.* 2013;33:347-53.

5. Mohler ER 3rd, Sarov-Blat L, Shi Y, Hamamdzic D, Zalewski A, MacPhee C, Llano R, Pelchovitz D, Mainigi SK, Osman H, Hallman T, Steplewski K, Gertz Z, Lu MM, Wilensky RL. Site-specific atherogenic gene expression correlates with subsequent variable lesion development in coronary and peripheral vasculature. *Arterioscler Thromb Vasc Biol.* 2008;28:850-5.

6. Wilensky RL, Shi Y, Mohler ER 3rd, Hamamdzic D, Burgert ME, Li J, Postle A, Fenning RS, Bollinger JG, Hoffman BE, Pelchovitz DJ, Yang J, Mirabile RC, Webb CL, Zhang L, Zhang P, Gelb MH, Walker MC, Zalewski A, Macphee CH. Inhibition of lipoprotein-associated phospholipase A2 reduces complex coronary atherosclerotic plaque development. *Nat Med.* 2008;14:1059-66.

7. Narula J, Nakano M, Virmani R, Kolodgie FD, Petersen R, Newcomb R, Malik S, Fuster V, Finn AV. Histopathologic characteristics of atherosclerotic coronary disease and implications of the findings for the invasive and noninvasive detection of vulnerable plaques. *J Am Coll Cardiol.* 2013;61:1041-51.

8. Asakura M, Ueda Y, Yamaguchi O, Adachi T, Hirayama A, Hori M, Kodama K. Extensive development of vulnerable plaques as a pan-coronary process in patients with myocardial infarction: an angioscopic study. *J Am Coll Cardiol.* 2001;37:1284-8.

9. Ohtani T, Ueda Y, Mizote I, Oyabu J, Okada K, Hirayama A, Kodama K. Number of yellow plaques detected in a coronary artery is associated with future risk of acute coronary syndrome: detection of vulnerable patients by angioscopy. *J Am Coll Cardiol.* 2006;47:2194-200.

10. Kubo T, Imanishi T, Kashiwagi M, Ikejima H, Tsujioka H, Kuroi A, Ishibashi K, Komukai K, Tanimoto T, Ino Y, Kitabata H, Takarada S, Tanaka A, Mizukoshi M, Akasaka T. Multiple coronary lesion instability in patients with acute myocardial infarction as determined by optical coherence tomography. *Am J Cardiol.* 2010;105:318-22.

11. Madder RD, Smith JL, Dixon SR, Goldstein JA. Composition of target lesions by near-infrared spectroscopy in patients with acute coronary syndrome versus stable angina. *Circ Cardiovasc Interv.* 2012;5:55-61.

12. Oemrawsingh RM, Cheng JM, Garcia-Garcia HM, van Geuns RJ, de Boer SP, Simsek C, Kardys I, Lenzen MJ, van Domburg RT, Regar E, Serruys PW, Akkerhuis KM, Boersma E; ATHEROREMO-NIRS Investigators. Near-infrared spectroscopy predicts cardiovascular outcome in patients with coronary artery disease. *J Am Coll Cardiol.* 2014;64:2510-8.

13. Kini AS, Baber U, Kovacic JC, Limaye A, Ali ZA, Sweeny J, Maehara A, Mehran R, Dangas G, Mintz GS, Fuster V, Narula J, Sharma SK, Moreno PR. Changes in plaque lipid content after short-term intensive versus standard statin therapy: the YELLOW trial (reduction in yellow plaque by aggressive lipid-lowering therapy). *J Am Coll Cardiol.* 2013;62:21-9.

14. Goldstein JA, Maini B, Dixon SR, Brilakis ES, Grines CL, Rizik DG, Powers ER, Steinberg DH, Shunk KA, Weisz G, Moreno PR, Kini A, Sharma SK, Hendricks MJ, Sum ST, Madden SP, Muller JE, Stone GW, Kern MJ. Detection of lipid-core plaques by intracoronary near-infrared spectroscopy identifies high risk of periprocedural myocardial infarction. *Circ Cardiovasc Interv.* 2011;4:429-37.

15. Pu J, Mintz GS, Biro S, Lee JB, Sum ST, Madden SP, Burke AP, Zhang P, He B, Goldstein JA, Stone GW, Muller JE, Virmani R, Maehara A. Insights into echo-attenuated plaques, echolucent plaques, and plaques with spotty calcification: novel findings from comparisons among intravascular ultrasound, near-infrared spectroscopy, and pathological histology in 2,294 human coronary artery segments. *J Am Coll Cardiol.* 2014;63:2220-33.

16. Kubo T, Maehara A, Mintz GS, Doi H, Tsujita K, Choi SY, Katoh O, Nasu K, Koenig A, Pieper M, Rogers JH, Wijns W, Böse D, Margolis MP, Moses JW, Stone GW, Leon MB. The dynamic nature of coronary artery lesion morphology assessed by serial virtual histology intravascular ultrasound tissue characterization. *J Am Coll Cardiol.* 2010;55:1590-7.

17. Zhao Z, Witzenbichler B, Mintz GS, Jaster M, Choi SY, Wu X, He Y, Margolis MP, Dressler O, Cristae E, Parise H, Mehran R, Stone GW, Maehara A. Dynamic nature of nonculprit coronary artery lesion morphology in STEMI: a serial IVUS analysis from the HORIZONS-AMI trial. *JACC Cardiovasc Imaging.* 2013;6:86-95.

18. Mintz GS, Nissen SE, Anderson WD, Bailey SR, Erbel R, Fitzgerald PJ, Pinto FJ, Rosenfield K, Siegel RJ, Tuzcu EM, Yock PG. American College of Cardiology Clinical Expert Consensus Document on Standards for Acquisition, Measurement and Reporting of Intravascular Ultrasound Studies (IVUS). A report of the American College of Cardiology Task Force on Clinical Expert Consensus Documents. *J Am Coll Cardiol.* 2001;37:1478-92.

19. Nicholls SJ, Tuzcu EM, Wolski K, Sipahi I, Schoenhagen P, Crowe T, Kapadia SR, Hazen SL, Nissen SE. Coronary artery calcification and changes in atheroma burden in response to established medical therapies. *J Am Coll Cardiol.* 2007;49:263-70.

20. Gardner CM, Tan H, Hull EL, Lisauskas JB, Sum ST, Meese TM, Jiang C, Madden SP, Caplan JD, Burke AP, Virmani R, Goldstein J, Muller JE. Detection of lipid core coronary plaques in autopsy specimens with a novel catheter-based near-infrared spectroscopy system. *JACC Cardiovasc Imaging.* 2008;1:638-48.

21. Virmani R, Kolodgie FD, Burke AP, Farb A, Schwartz SM. Lessons from sudden coronary death: a comprehensive morphological classification scheme for atherosclerotic lesions. *Arterioscler Thromb Vasc Biol.* 2000;20:1262-75.

Supplementary data

Appendix. Imaging protocol.

Appendix Figure 1. Chemograms and histology of a right coronary artery obtained from an animal that died suddenly between the three- and six-month diagnostic evaluations.

Appendix Figure 2. NIRS, IVUS, histology of culprit lesion in animal suffering sudden death 42 days after three-month NIRS/IVUS evaluation.

Supplementary data

Appendix. Imaging protocols

IVUS ANALYSIS

All IVUS images (1 mm apart) were analysed in diastole and analysis was performed according to the clinical consensus document on IVUS[18]. Plaque plus media (P+M) area was determined by subtracting the luminal cross-sectional area from the external elastic lamina cross-sectional area. Echo-attenuated plaque (AP) area was measured and defined as the hypoechoic area within external elastic lamina boundaries. Total arterial atheroma area was estimated by summation of each P+M cross-sectional area (mm^2) over the length of the artery. Total arterial AP area was estimated in a similar fashion. For each TCFA, an IVUS-derived remodelling index was calculated. If the lesion external elastic lamina area was greater than a reference external elastic lamina area, positive remodelling had occurred. Remodelling index <1 indicated negative remodelling. The reference external elastic lamina was defined as the largest external elastic lamina area within a 5 mm distance proximal or distal to the lesion. Calcification was assessed by two methods. For each measured image, a calcium grade was assigned which reflected the presence of calcium and degree of acoustic shadowing (0=no calcium, 1=calcium with acoustic shadowing <90°, 2=calcium shadowing ≥90°)[19]. If an image contained multiple calcium deposits, a grade was assigned after summation of all the angles of acoustic shadowing. A per-vessel calcium index for each pullback was derived by calculating the average calcium grade of all images. The degree of calcification was also expressed as the percent of artery containing any calcium.
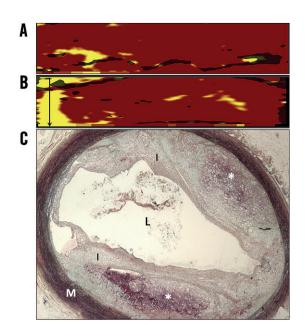
NIRS ANALYSIS

The algorithm to detect lipid core plaque and derive a block chemogram for NIRS scans has been previously described and validated in *ex vivo* human coronary arteries[20]. For each pullback a chemogram, a block chemogram, and a lipid core burden index (LCBI) were determined. The probability of lipid core plaque for each scanned segment was displayed as a two-dimensional spatial map, or chemogram, with the x-axis indicating region of interest in millimetres, and the y-axis the circumferential position (0°-360°). On the chemogram, the algorithm displayed the probability of lipid core plaque at the region of interest by using a colour scale where each pixel marked red indicated low probability and each yellow pixel a high probability. The block chemogram provided a summary of data to enhance interpretation of the chemogram and displayed the probability that lipid core plaque was present for all measurements using the top 10th percentile pixel information of the corresponding 2 mm chemogram segment. If the algorithm probability was ≥0.98 that a lipid core plaque was present in that 2 mm block, the entire block was assigned yellow. The LCBI denotes the extent of lipid core plaque over the entire scanned artery segment computed as the fraction of valid pixels within the scanned region that exceeded a lipid core plaque probability of 0.6, multiplied by 1,000.

TISSUE RETRIEVAL AND HISTOLOGICAL ANALYSIS

All sections were stained with Movat's pentachrome while adjacent 5 μm sections containing fibroatheromas were stained with Picro-sirius red. Picro-sirius red more clearly delineates the fibrous cap thickness by assessing collagen's birefringence under a polarising light source[4].

Sections were quantitatively analysed using Image-Pro Plus (Media Cybernetics, Rockville, MD, USA) to measure the P+M, intimal and necrotic core areas. The necrotic core was defined as those areas in which extracellular matrix was absent and replaced by necrotic debris using Movat's and Picro-sirius red staining. The thickness of the thinnest cap segment was determined by Picro-sirius staining. From the Movat's stained sections, fibroatheroma depth was assessed in two ways. Depth was measured from both the intimal border and the central point of the arterial lumen to the deepest abluminal TCFA edge. Sections were then classified using the modified AHA classification by two independent observers, blinded to both the IVUS and NIRS data, as either TCFA, thick-cap fibroatheroma (ThCFA), or non-fibroatheromas (pathological intimal thickening, intimal hyperplasia, and normal tissue)[21].

TCFAs were defined as having a fibrous cap <100 μm.

Appendix Figure 1. *Chemograms and histology of a right coronary artery obtained from an animal that died suddenly between the three- and six-month diagnostic evaluations. A) Chemogram and block chemogram measured in vivo at three months. B) Post mortem chemogram and block chemogram obtained ex vivo. The quantity of NIRS-derived lipid core plaque increased between the three-month evaluation and the time of the animal's sudden cardiac death, particularly in the proximal region of interest. Black arrow identifies region of interest in which a TCFA was detected at necropsy. C) Movat's pentachrome stain of a TCFA detected at necropsy within the proximal right coronary artery with a thin fibrous cap over two areas of dense necrotic core containing intraplaque haemorrhage. Area of the lipid core plaque corresponds to the presence of a TCFA at necropsy. *necrotic core; I: intima; L: lumen; M: media; NIRS: near infrared spectroscopy; TCFA: thin-cap fibroatheroma*

Appendix Figure 2. *NIRS, IVUS, histology of culprit lesion in animal suffering sudden death 42 days after three-month NIRS/IVUS evaluation. A) Chemogram and block chemogram measured in vivo at three months. Black arrow identifies region of interest in which a coronary thrombosis was detected at necropsy. B) IVUS of region of interest. Culprit lesion is outlined. Note the substantial increase in lesion severity between the IVUS and death. C) Movat's pentachrome stain of culprit coronary artery lesion notable for lumen thrombosis and atherosclerosis. *thrombus; I: intima; IVUS: intravascular ultrasound; NIRS: near infrared spectroscopy*